J. Microbiol. Biotechnol. (2016), 26(3), 530–539
http://dx.doi.org/10.4014/jmb.1510.10040

jmb

FMN-Based Fluorescent Proteins as Heavy Metal Sensors Against Mercury Ions

Yuvaraj Ravikumar[1], Saravanan Prabhu Nadarajan[2], Chong-Soon Lee[1], Seunho Jung[2], Dong-Ho Bae[2], and Hyungdon Yun[2]*

[1]*School of Biotechnology, Department of Biochemistry, Yeungnam University, Gyeongsan 38541, Republic of Korea*
[2]*Department of Bioscience and Biotechnology, Konkuk University, Seoul 05029, Republic of Korea*

Received: October 14, 2015
Revised: December 9, 2015
Accepted: December 14, 2015

First published online
December 23, 2015

**Corresponding author*
Phone: +82-2-450-0496;
Fax: +82-2-450-4769;
E-mail: hyungdon@konkuk.ac.kr

pISSN 1017-7825, eISSN 1738-8872

Bacterial light-oxygen-voltage-sensing photoreceptor-derived flavin mononucleotide (FMN)-based fluorescent proteins act as a promising distinct class of fluorescent proteins utilized for various biomedical and biotechnological applications. The key property of its independency towards oxygen for its chromophore maturation has greatly helped this protein to outperform the other fluorescent proteins such as GFP and DsRed for anaerobic applications. Here, we describe the feasibility of FMN-containing fluorescent protein FbFP as a metal-sensing probe by measuring the fluorescence emission changes of a protein with respect to the concentration of metal ions. In the present study, we demonstrated the mercury-sensing ability of FbFP protein and the possible amino acids responsible for metal binding. A ratiometric approach was employed here in order to exploit the fluorescence changes observed at two different emission maxima with respect to Hg^{2+} at micromolar concentration. The engineered variant $FbFP_{C56I}$ showed high sensitivity towards Hg^{2+} and followed a good linear relationship from 0.1 to 3 μM of Hg^{2+}. Thus, further engineering with a rational approach would enable the FbFP to be developed as a novel and highly selective and sensitive biosensor for other toxic heavy metal ions as well.

Keywords: FbFP protein, ratiometric, fluorescence quenching, mercury

Introduction

In the present decade, the presence of heavy metals in the environment as a harmful environmental pollutant has started to cause a serious threat to the welfare of human beings and other organisms. Among the various heavy metals, mercury (one of the most common heavy metal contaminant) can induce adverse effects to the organ system, in particular to the nervous system and accompanied with cognitive dysfunctions as well [9, 10]. Therefore, in order to control or manage the adverse health and environmental effects, developing probes to detect the trace amount of Hg^{2+} is of utmost importance. The current traditional approaches for qualitative and quantitative analyses of Hg^{2+} broadly utilizes the analytical-based instruments such as atomic absorption spectroscopy and inductive-coupled plasma mass spectrometry [25]. Although the above two methods offer high sensitivity, the laborious sample preparation process and also the sample loss during analysis make them unsuitable for wider applications. Therefore, it would be highly commendable to develop methods that in turn can exploit cheap portable devices for easy and efficient on-field detection of Hg^{2+}. To address this challenge, more recently, fluorescent proteins-based metal sensors have emerged as a simpler and straightforward strategy for developing biosensors against heavy metals [23].

The extensive studies on genetically encoded fluorescent proteins such as GFP, DsRed, YFP and, others have led researchers to exploit these proteins for various successful functional applications [8, 24]. Furthermore, protein engineering tools like rational mutagenesis and directed evolution approaches have made a significant contribution to the development of numerous novel fluorescent probes

that can be potentially used for cell imaging and visualization studies [5]. For instance, the engineered long Stokes shift red fluorescent protein has enabled researchers to detect the in vivo Ca^{2+} changes in neuronal cells [26]. In addition, the engineering of GFP with histidine and introduction of metal-binding residues in and around the chromophore region have led to the development of an efficient Cu^{2+} sensor [2]. Similarly, engineering the GFP chromophore with Cys enables the protein to sense toxic heavy metals such as Pb^{2+} and Hg^{2+}, respectively [4, 18]. With such great demand, the search of new fluorescent proteins for metal-sensing applications keeps constantly growing. More recently, many new fluorescent proteins from aquatic marine organisms have been characterized successfully and utilized for biosensing applications. For instance, the first report by using far-red fluorescent protein as a reagentless-based Cu^{2+} sensor was derived from *Heteractis crispa* [20]. Similarly, recombinant GFP isolated from *Anemonia sulcata* has enabled the researchers to sense the very low concentration of Cu^{2+} and Hg^{2+} in a sensitive manner [15]. Further to expanding the metal-sensing applications, in the last few years, an unnatural amino acid incorporation tool was exploited effectively to generate sensors that could be able to detect Cu^{2+}, Mn^{2+}, and so on, respectively [1, 13].

Despite the wide range of fluorescent proteins reported for metal-sensing applications, most of the fluorescent proteins like GFP and others strictly require molecular oxygen for their chromophore formation, which hinders its utility towards low-oxygen condition environment applications. More recently, a family of blue-light photoreceptor proteins containing light-oxygen-voltage (LOV)-sensing domain fluorescent proteins is emerging as a better candidate for more successful functional applications [3, 16]. In particular, for metal-sensing applications, a flavin mononucleotide (FMN) chromophore-based iLOV protein was recently utilized for developing a copper sensor [21]. In this report, we were interested in exploring a new class of fluorescent proteins called flavin-binding fluorescent proteins (FbFP) for metal-sensing applications. These FMN-based fluorescent proteins have distinct advantages over the oxygen-dependent fluorescent proteins. The most important one is the rapid and oxygen-independent chromophore maturation, which allows this protein to be exploited for a wide range of applications that can work effectively under anaerobic conditions [6]. In addition, the presence of two emission maxima, the chromophore maxima at 495 nm and the shoulder maxima at 520 nm, due to the presence of FMN seems to be ideal for its use as a ratiometric probe [16]. From this perspective, we hereby demonstrate the ability of the FMN-based FbFP for the metal-sensing purpose, and also for the first time, we show how engineering the key residues near the chromophore can lead to the development of a reagentless- and ratiometric-based fluorescent probe against mercury ions.

Materials and Methods

Construction of Plasmids and Strains

The host bacterium *Escherichia coli* (*E. coli*) strain XL1-blue (Stratagene, CA, USA) was utilized for preparing the plasmid DNA. The plasmid-containing *E. coli* cells were grown in Luria-Bertani (LB) broth (Difco Labororatories, Detroit, MI, USA) under aerobic conditions or on LB agar plates supplemented with appropriate antibiotics for the transformant selection. The pQE80L plasmid and the nickel-nitrilotriacetic acid (Ni-NTA) affinity column were purchased from Qiagen (Valencia, CA, USA). Isopropyl-L-D-thiogalactopyranoside (IPTG) (Carbosynth) and all the other chemicals used were purchased from Sigma-Aldrich, Korea. The *Pseudomonas putida* KT2440 gene coding for the FbFP (RefSeq ID: NP_744883.1) was chemically synthesized after codon optimization to comply with the codon preferences of *E. coli* (Bioneer Inc., Daejon, South Korea) [17]. The synthetic gene was supplied by Bioneer Inc. after cloning into the pGEm-T easy vector (Promega, Madison, WI, USA). The synthetic FbFP gene was cut with the restriction enzymes BamHI and HindIII and then inserted into the IPTG-inducible expression vector pQE80L. The plasmid was further transformed into the *E. coli* (BL21) cells.

Amino Acid Sequence of FbFP

MRGSHHHHHHGSMSPMINAKLLQLMVEHSNDGIVVAEQE
GNE**S**ILIYVNPAFERLTGYCADDILYQD**C**RFLQGEDHDQPGIAI
IREAIREGRPCCQVLRNYRKDGSLFWNELSITPVHNEADQLTY
YIGIQRDVTAQVFAEERVRELEAEVAELRRQQGQAKH

In this sequence information, two amino acids are highlighted in bold font and underlined. Ser31 and Cys56 were mutated into Cys and Ile, respectively.

Molecular Modeling Studies

A BLASTP search was performed against the protein sequence of FBFP. Based on the sequence alignment, the best template for FbFP, bacterial photoreceptor protein (PDBID 3SW1), was utilized for 3D modeling using a homology modeler. The modeled 3D structure was verified using the SAVES server. The modeled 3D structure was also analyzed for mutation with metal-binding amino acids His, Cys, Asp, and Glu, using Pymol. The model structure was screened for the evolutionary profile of amino acids using the online tool Consurf database.

Site-Directed Mutagenesis

The pQE80L plasmid containing FbFP was used for generating

variants such as $FbFP_{S31C}$ and $FbFP_{C56I}$. The mutants were generated from the FbFP by using a Quick-exchange site-directed mutagenesis kit (Stratagene) according to the manufacturer's description manual. The mutagenesis was confirmed by DNA sequencing analysis at Cosmo Genetech, Daejeon, South Korea.

Protein Expression and Purification

The BL21 transformants containing the pQE80L-FbFP and variants were grown at 37°C in 1 L of LB broth containing 100 μg/ml of ampicillin. When the absorbance reached to 0.6 at OD_{600}, the protein expression was induced by adding IPTG to a final concentration of 1 mM. The culture was then incubated at 37°C. After 7 h of induction, the cells were harvested, washed, and subjected for centrifugation and were then stored at −80°C for further use. The cell pellets were then resolubilized in 5 ml of lysis buffer (300 mM NaCl and 5 mM imidazole) at pH 7.0. The cells were subjected to ultrasonic disruption for 20 min, followed by centrifugation at 28,000 ×*g* for 30 min at 4°C. The soluble fraction containing the target proteins were further purified at 4°C by using Ni-NTA agarose resin (GE Healthcare Bio-Sciences, Sweden) as directed in the manufacturer's manual. The eluted fractions were then analyzed by SDS-PAGE and were further dialyzed against 1× phosphate-buffered saline. The concentration of the purified protein was quantified using the Bradford assay.

Metal-Sensing Assay

As an initial study, FbFP and its variants were screened with different metal ions in order to identify any specific affinity for the selective binding of metal ions. All the metal ions used in this study were freshly prepared in deionized triple-distilled water. To test this, 100 μl of final concentration of 3 μM FbFP and its variants were prepared in 20 mM MOPS buffer at pH 7.4 and treated with the equal volume containing 200 μM of metal ions. After incubating the samples for 30 min at 25°C, the samples were excited at 450 nm and the emitted fluorescence was measured at 495 nm.

Mercury Titration and Ratiometric Analysis

To analyze the Hg^{2+} binding, 100 μl of mercury solution at different concentrations (0−10 μM) was added to 100 μl of final concentration of 3 μM FbFP and $FbFP_{C56I}$ (in 20 mM MOPS buffer at pH 7.4). Fluorescence measurements were recorded and baseline corrected. The graph was plotted by taking ratiometric values obtained from 520 nm/495 nm against different Hg^{2+} concentrations. The samples were excited at 450 nm and the fluorescence emission was recorded at 495 and 520 nm, respectively.

CD-Spectroscopy Analysis

A far UV CD spectrum was measured for the FbFP and $FbFP_{C56I}$ variant by using a Jasco J-715 spectrophotometer. For the analysis, 3 μM of protein samples were placed in a 0.2 cm cell and the absorption spectrum was recorded at room temperature. Furthermore, a final concentration of 3 μM Ba^{2+} and Hg^{2+} was added separately and the absorbances were recorded. Five scans were accumulated per spectrum and raw data were analyzed using the Jasco software package.

Results and Discussion

Flavin-binding protein utilizes external cofactor FMN as it chromophore, which emits fluorescence at 495 nm and has a shoulder peak at 520 nm. In this study, we planned to characterize the inherent metal-binding property of FbFP and engineer a mercury-sensing FbFP. It is well known that the four amino acids His, Cys, Asp, and Glu enable metal-binding properties to the proteins. In addition, the backbone carbonyl atom of all amino acids and the free hydroxyl-containing amino acids such as Ser, Thr, and Tyr of proteins help in coordinating metal ions in all metal-binding protein. To characterize and engineer the metal-binding site, we have to analyze the amino acids residing near the chromophore of FbFP and introduce these metal-binding amino acids near the chromophore. Since there is no three-dimensional (3D) structure for our target protein, we constructed a 3D model structure for FbFP using a bacterial photoreceptor (3SW1) as a template structure. Based on the model, we analyzed the metal-coordinating amino acids residing near the chromophore. Similar to the FMN-dependent fluorescent protein (iLOV protein), the FMN chromophore of FbFP is completely surrounded by Asn, Glu, and Arg. From the 3D model structure, we observed two probable metal-binding sites (site 1 and site 2) that can be utilized for engineering heavy metal sensors (Fig. 1). Site 1 metal binding contains Asp and Ser residing near to the FMN, which coordinates to the water as seen in the crystal structure PBDID-3SW1. Site 2 contains Cys at the 56^{th} position, whose free thiol is facing towards the phenyl ring of FMN (Fig. 1). To engineer metal-sensing FbFP, we planned to construct the model by mutating the Asp55, Ser31, and Cys56 with His, Cys, Asp, and Glu (Fig. 2). In general, the amino acids residing near the chromophore are highly conserved; mutating these residues with other residues ends with fluorescent loss or change in spectral features. In order to prevent the fluorescent loss, we analyzed evolutionarily conserved profiles of amino acids in FbFP using the Consurf Database and utilized the conserved metal-binding amino acid for modeling (Table 1). Among the three residues, the Asp55 is a highly conserved amino acid and replacing it with another amino acid will have deleterious effect such as loss of fluorescence and solubility. Thus, we planned to mutate Ser31 with His, Asp and Glu, Cys, where except for Cys all other flip away from

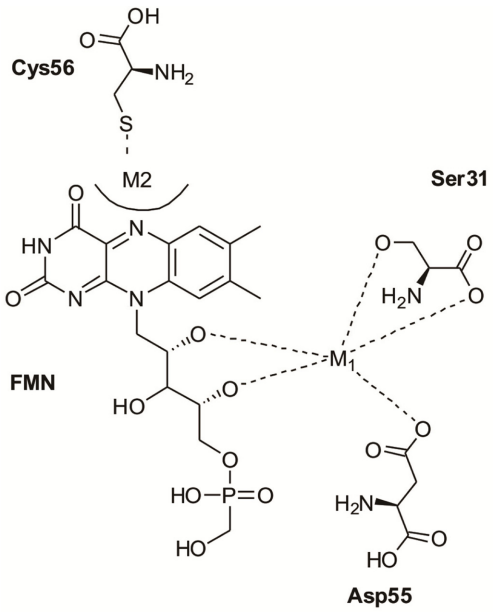

Fig. 1. Probable metal-binding sites of FbFP.
2D structural analysis representing the probable metal-binding sites of FbFP residing closer to the chromophore FMN. M1 represents the metal-binding site 1, which might be coordinated between the sidechain carboxyl atom of Asp55 and carbonyl oxygen of Ser31 along with FMN. M2 represents metal-binding site 2, in which the free thiol group of Cys56 bound to the metal ions can create steric hindrance to the FMN.

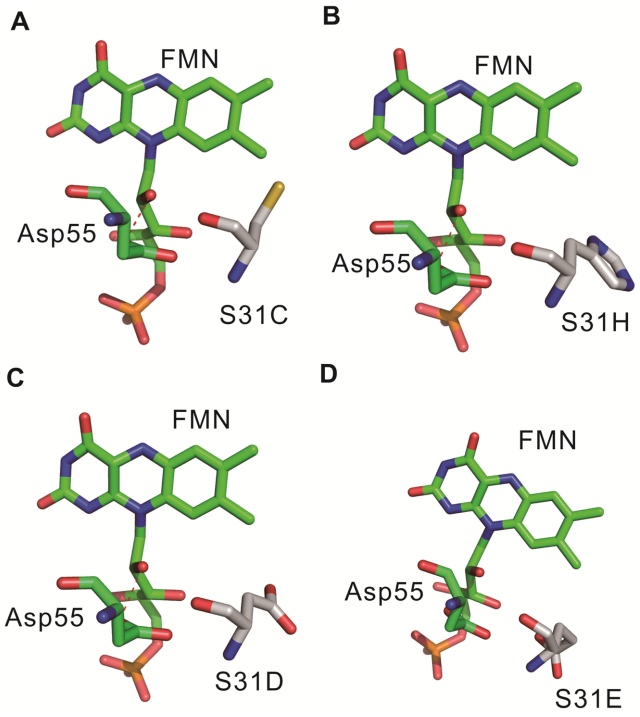

Fig. 2. Structural analysis of homology modeled FbFP.
Structural modeling of Ser31 of FbFP with Cys, His, Asp, and Glu represented as (**A**) S31C, (**B**) S31H, (**C**) S31D, and (**D**) S31E.

Table 1. Conserved amino acids analyzed through CONSURF database.

Amino acid	Conserved amino acids
Serine 31	C,S,H,E,W,V,K,D,M,T,Y,Q,L,N,P
Aspartic acid 55	D,T,N,P
Cysteine 56	I,P,L,T,G,V,W,F,S,C

the metal-binding site. On the other hand, we planned to engineer the Cys56 with a metal-binding amino acid but it is conserved with a hydrophobic amino acid, and we planned to alter the metal-binding site 2. Thus, we constructed two different mutants, $FbFP_{S31C}$ and $FbFP_{C56I}$, by mutating Ser31 into Cys and Cys56 into Ile, respectively.

Protein Expression and Purification

The plasmid bearing the gene for FbFP and its variants was cloned into the T5 promoter containing the pQE80L vector. The BL21 cells harboring the FbFP and its variants upon IPTG induction produced good protein expression, which was greenish in color. The expressed proteins were then purified using the Ni-NTA affinity column. The nonspecifically bound proteins were removed by using 5 mM imidazole containing wash buffer. The purified protein fractions were then collected and dialyzed overnight against 1× PBS buffer in order to remove imidazole completely. The proteins that were now imidazole free were subjected to concentration by using an Amicon PM-10 ultrafiltration unit and then stored at 4°C until further use. The purified proteins were checked by SDS-PAGE analysis which gave a single clear band on the gel (Fig. 3).

Metal-Screening Assay

As an initial study, the emission spectra were recorded for all the purified proteins, including wild-type FbFP and its variants $FbFP_{S31C}$ and $FbFP_{C56I}$ (Fig. 4). All the proteins exhibited characteristic emission spectra and were similar to that of the earlier reports, comprising two emission peaks, one at 495 nm and the other being the FMN peak at 520 nm [6]. Later, to interrogate the effect of a broad range of physiologically active and environmental-related hazardous-causing heavy metal ions, the purified proteins were screened for metal selectivity in the presence of different monovalent and bivalent metal ions. Final concentrations of these metal ions were prepared and used for the

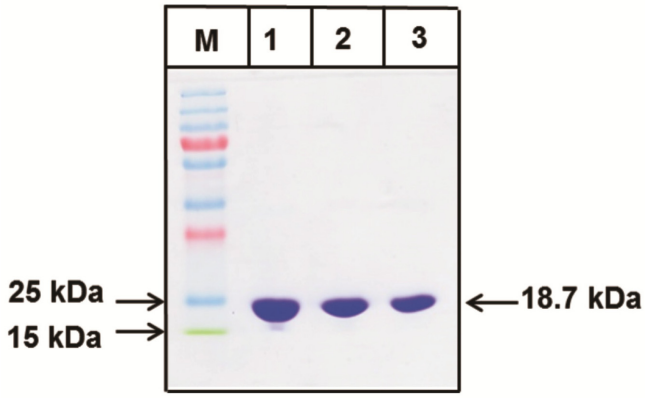

Fig. 3. SDS-PAGE analysis of purified FbFP protein and its mutants.

Lane M represents the molecular weight marker. Lane 1 represents the purified FbFP; Lane 2, $FbFP_{S31C}$ and Lane 3, $FbFP_{C56I}$ protein after Ni-NTA affinity chromatography.

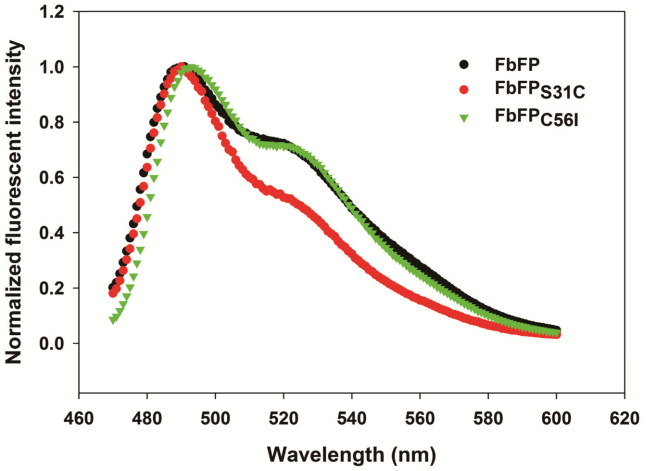

Fig. 4. Emission spectra of FbFP and its variants.

Fluorescence emission spectra were measured by exciting at 450 nm. A final concentration of 3 μM FbFP and its variants were prepared in 20 mM MOPS buffer at pH 7.4.

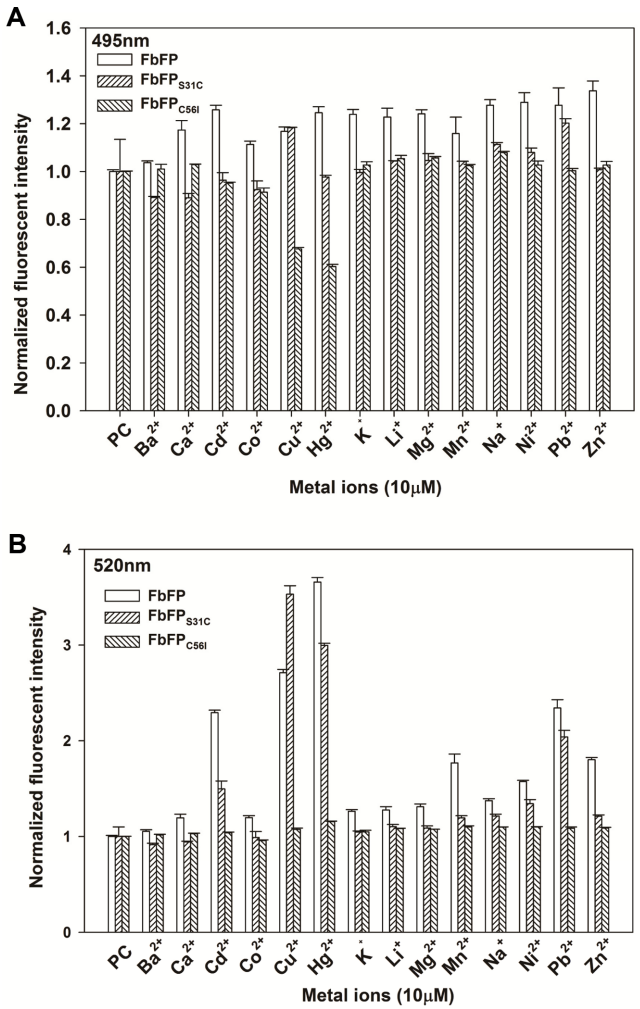

Fig. 5. Metal selectivity assay of FbFP and its mutants with different metal ions.

(**A**) Bar chart representing the fluorescent emission intensities recorded at 495 nm by exciting the sample at 450 nm. Values represent the mean ± SD ($n = 3$). (**B**) Bar chart representing the fluorescent emission intensities recorded at 520 nm by exciting the sample at 450 nm. A final concentration of 3 μM proteins (20 mM MOPS buffer, pH 7.4) was incubated with 10 μM of metal ions for 30 min. Values represent the mean ± SD ($n = 3$).

analysis. Emission spectra in the presence and absence of metal ions were recorded by excitation at the maximum excitation wavelength of FbFP and its mutants. The results showed that the addition of Ba^{2+}, Ca^{2+}, K^{+}, Li^{+}, Mg^{2+}, Mn^{2+}, and Na^{+} did not affect the fluorescence emission of FbFP at 495 nm, whereas the heavy metal ions such as Hg^{2+} and Cu^{2+} showed a significant fluorescence quenching at 495 nm with both FbFP and its variant $FbFP_{C56I}$ (Fig. 5A). Interestingly, an increase in fluorescence emission at 520 nm was found with the other heavy metals Cu^{2+}, Cd^{2+}, Pb^{2+}, and Zn^{2+} in both the wild type and $FbFP_{S31C}$ (Fig. 5B).

The addition of mercury with the $FbFP_{S31C}$ mutant enabled a fluorescence emission shift at 520 nm. It is also quite surprising that metal ions such as Ba^{2+} and Ca^{2+} do have an effect on the fluorescence quenching with the $FbFP_{S31C}$ mutant. Based on the different model structures, it is clear that the sidechain thiol group of Cys31 flips towards the other side. It depicts that the backbone carboxylic atom of the amino acid at 31 is involved in coordinating metal along with FMN and Asp55, and mutating Ser31 with another amino acid will not enable a successful metal-

binding site. Meanwhile, it is worth noting that the $FbFP_{C56I}$ mutant did not have any pronounced changes in fluorescence at 520 nm against mercury (Fig. 5B). Furthermore, as the S31C mutant in the wild type failed to show fluorescence quenching with respect to metals, we analyzed $FbFP_{C56I}$. Mutation of Cys56 with Ile enabled fluorescence quenching with respect to mercury. Since Cys56 is adjacent to Asp55, mutation of Cys with Ile might enable proper orientation of Asp55. Furthermore, we carried out the metal sensing characterization with $FbFP_{C56I}$ mutant. On the basis of the obtained initial results, our observations lend support to the notion that a change in the fluorescent emission of $FbFP_{C56I}$ was possibly mediated by metal-catalyzed fluorescent quenching. In general, among various heavy metal ions, mercury is considered as one of the most important metal ions because of its interesting properties. Despite of its toxic nature, cinnabar (containing HgS) has been widely used as a traditional Chinese medicine for centuries [7]. More recently, its use in amalgam fillings for dental applications has been considerably increasing [14]. However, the slow release from use of such amalgams can cause ill-effects to renal, neurological, and other physiological problems as well [14]. With such high significance towards mercury, and given that substitution of Cys56 with Ile made the FbFP considerably more sensitive for fluorescent decrease by Hg^{2+} ions, it is reasonable to conclude that this improvement might be due to binding of Hg^{2+} ions to the protein chromophore.

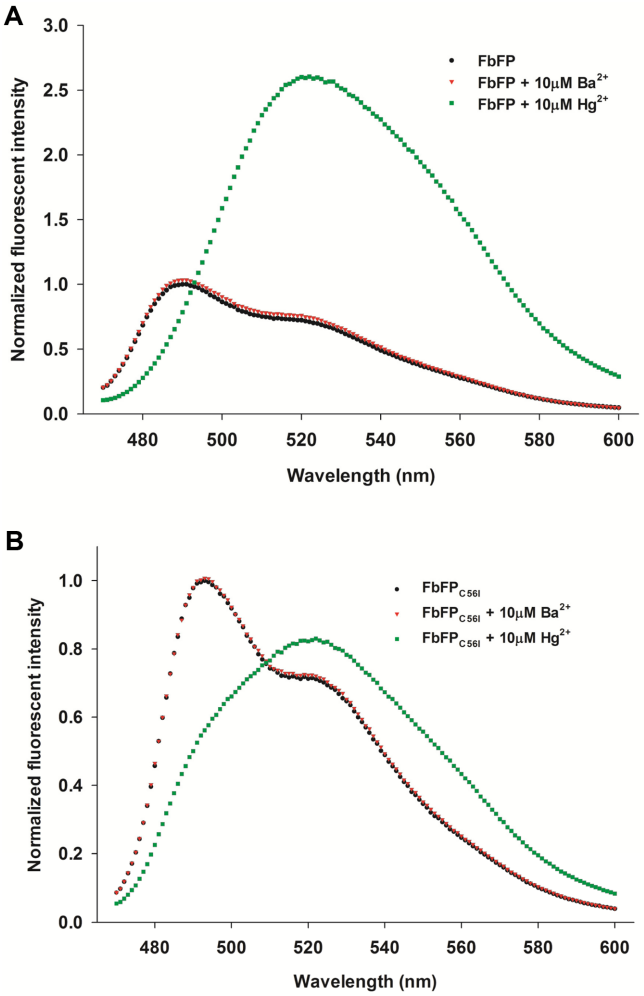

Fig. 6. Changes in the fluorescence emission intensity of FbFP and $FbFP_{C56I}$.

(**A**) Plot showing changes in fluorescence of FbFP against 10 μM Ba^{2+} and 10 μM Hg^{2+}. (**B**) Plot showing changes in fluorescence of $FbFP_{C56I}$ against 10 μM Ba^{2+} and 10 μM Hg^{2+}. A final concentration of 3 μM FbFP and $FbFP_{C56I}$ was dissolved in 20 mM MOPS buffer (pH 7.4) and incubated for 30 min and emission spectra were recorded.

Mercury-Binding Study

The ability of FbFP and $FbFP_{C56I}$ to recognize Hg^{2+} was demonstrated through detailed investigation by recording a full emission spectrum in a wavelength ranging from 470 to 600 nm. From Figs. 5A and 5B, fluorescence in the emission spectrum at 520 nm was highly increased in the wild type, whereas the mutant did not produce any profound changes at 520 nm when treated with 10 μM Hg^{2+}. To confirm that these changes arise only due to the Hg^{2+} interaction, we also examined the effect of the fluorescence emission in the presence of 10 μM Ba^{2+}. The observed results with no distinguishable changes in fluorescence emission at both 495 and 520 nm strongly suggest that Ba^{2+} did not interact with the chromophore whereas Hg^{2+} interacted with the protein chromophore (Figs. 6A and 6B). As described earlier in the previous reports, the 495 nm fluorescence originates from the protein itself and the 520 nm fluorescence is due to the presence of FMN. Thus, from this perspective, the results suggest that binding of Hg^{2+} at the protein chromophore of the mutant is responsible for the fluorescence quenching at 495 nm. With such interesting results, we next planned to investigate the extent of fluorescence quenching by titrating both the wild-type FbFP and $FbFP_{C56I}$ against different concentration of Hg^{2+} ions.

CD Spectroscopy Study

To investigate the mechanism of fluorescence quenching by mercury ions, measurement of CD spectra for FbFP and $FbFP_{C56I}$ with the addition of metal was performed. In the absence of metal ions, both the proteins maintained their

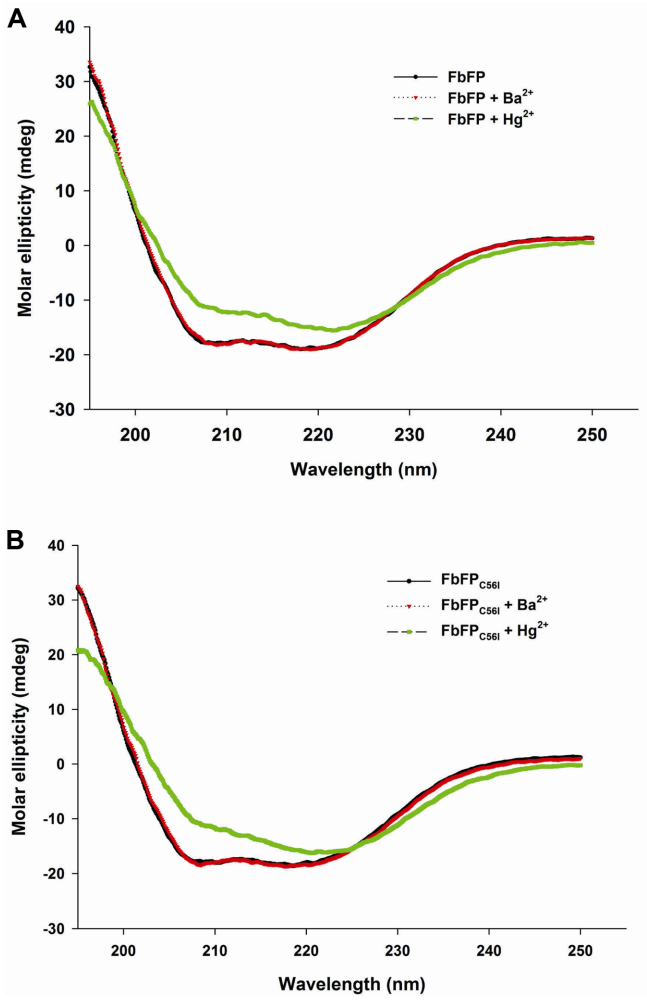

Fig. 7. CD spectroscopic analysis.

(**A**) Graph illustrating the secondary structure analysis of FbFP in the presence and absence of Ba^{2+} and Hg^{2+} ions. (**B**) Graph illustrating the secondary structure analysis of $FbFP_{C56I}$ in the presence and absence of Ba^{2+} and Hg^{2+} ions. The protein samples to a final concentration of 3 μM were prepared in 20 mM MOPS buffer (pH 7.4) and were treated with similar concentration of metal ions, respectively.

secondary structure by exhibiting the characteristic spectral profile as similar to other proteins. In general, the α-helix structure is represented as a positive band at 192 nm and negative bands at 195 and 216 nm, respectively. Moreover, the β-sheet exhibits a negative band at 218 nm and a positive one at 196 nm [12]. Based on the above described comments, in both FbFP and $FbFP_{C56I}$, the α-helix and β-sheets patterns were well matched in the presence of 3 μM Ba^{2+} (Figs. 7A and 7B). However, with respect to Hg^{2+}, both the wild-type FbFP and $FbFP_{C56I}$ showed pronounced changes in the secondary structure during analysis. The intensity of the CD spectral bands was significantly reduced at both the α-helix and β-sheets regions of the proteins when treated with mercury ions. Taken together with the aforementioned result on fluorescent changes as shown in Fig. 6, it can be suggested that the changes that occurred in the fluorescent emission as a result of Hg^{2+} ions may be due to metal-binding induced structural changes. In addition, with respect to changes observed at the α-helix and β-sheets, it suggests that in the presence of Hg^{2+} ions, some conformational or structural changes may also have taken place (Figs. 7A and 7B).

Hg^{2+} Titration Study

Sensitivity is an important parameter for developing efficient probes towards metal ions. With regard to mercury ions, earlier reports have shown that engineering the fluorescent proteins can enable such fluorescent probes to act as a highly sensitive mercury sensor. For example, single substitution of amino acid Ser205 into Cys in GFP exhibited a selective and sensitive fluorescence quenching towards mercury with a detection limit of 2 nM [4]. More recently, with a similar kind of strategy, GFPxm (a variant derived from fluorescent protein from *Aequorea macrodactyla*) bearing a single point mutation at His 148 with Cys enabled the protein to give a turn-on fluorescence and also demonstrated the ability to detect Hg^{2+} within the live cells [11]. In this report, to analyze the sensitivity of $FbFP_{C56I}$ with respect to Hg^{2+}, a titration study was performed by adding different concentrations of Hg^{2+} (0.1–10 μM Hg^{2+}) to both the wild-type and FbF_{C56I} proteins. Dose-response curves were further generated by plotting the fluorescence change of FbFP and $FbFP_{C56I}$ against different concentrations of mercury ions. The protein samples with mercury were incubated for 30 min at room temperature and the fluorescence intensities at both 495 and 520 nm were recorded. On the basis of Fig. 8, it clearly shows the wild-type FbFP did not produce any fluorescence quenching at 495 nm, whereas the mutant protein showed an excellent linear-based fluorescent quenching towards Hg^{2+} ranging from 0.1 to 10 μM. Similarly, with respect to FMN chromophore-based fluorescence at 520 nm, there were not any substantial differences in the mutant protein, whereas the wild type exhibited a dramatic increase fluorescence exponentially as the concentration of Hg^{2+} is increased. This might be due to the interaction of Hg^{2+} with the protein, causing the FMN to be released via some conformational changes, which in turn led the free FMN to produce fluorescence enhancement at 520 nm. Altogether, the sensitivity against mercury (0.1–3 μM) was highly

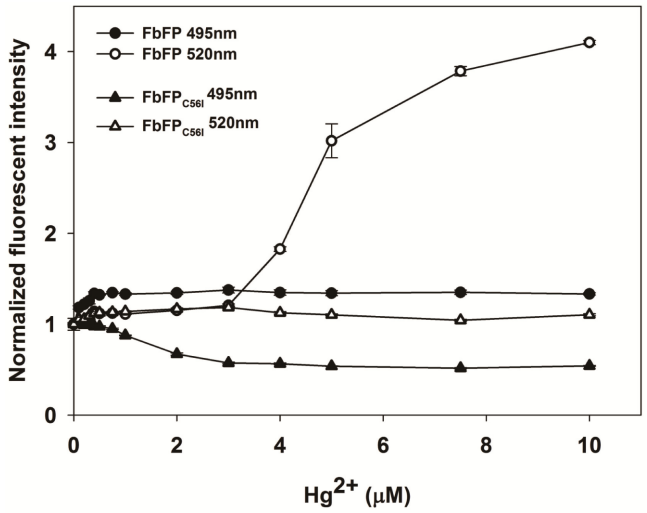

Fig. 8. Mercury titration curve analysis.
Plot showing the changes in the fluorescence emission intensity of FbFP and FbFP$_{C56I}$ against different Hg^{2+} concentrations (0.1 μM–10 μM). The 6 μM FbFP and FbFP$_{C56I}$ were dissolved in 20 mM MOPS buffer (pH 7.4) and incubated for 30 min and emission spectra were recorded by exciting the sample at 450 nm. Values represent the mean ± SD (n = 3).

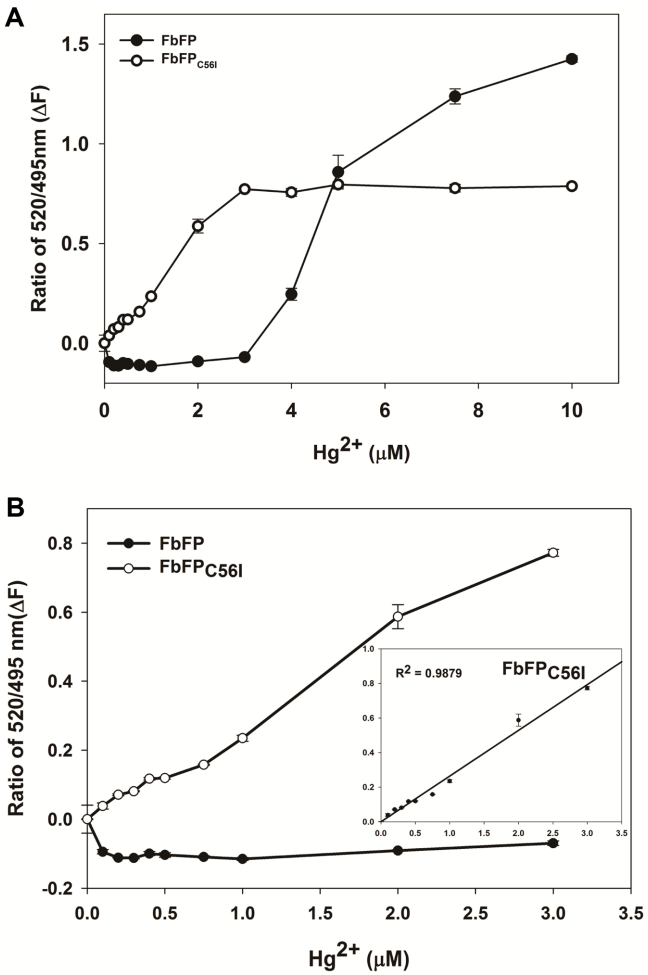

Fig. 9. Ratiometric analysis of FbFP and FbFP$_{C56I}$ with mercury ions.
(**A**) Plot showing the ratiometric analysis of fluorescence emission changes of FbFP and FbFP$_{C56I}$ against different Hg^{2+} concentrations (0.1–10 μM). (**B**) Plot showing the linear relationship of ratiometric-based fluorescence emission changes of FbFP and FbFP$_{C56I}$ until 3 μM Hg^{2+} ions. A final concentration of 3 μM protein samples was prepared in 20 mM MOPS buffer (pH 7.4) and incubated for 30 min and emission spectra were recorded. Here, ΔF is the change in the measured fluorescence in the presence of Hg^{2+} recorded at 495 and 520 nm by exciting the sample at 450 nm. Values represent the mean ± SD (n = 3).

remarkable, making it ideal to suggest the mutant as a potential probe.

Ratiometric-Based Fluorescence Analysis

With the observed results, we further intended to exploit the differences observed in the emission intensity at both peaks with wild type and mutant, so that it could be utilized for ratiometric analysis with respect to Hg^{2+} ions. The huge advantage of using a ratiometric sensor over the non-ratiometric is that a non-ratiometric-based fluorescent biosensor used for metal-sensing applications has certain limitations, especially towards live-cell imaging and microscopic studies. The reasons are likely because the fluorescent intensity from the non-ratiometric means is dependent on many external factors, like acquisition conditions, probe concentration, and optical path length. However, a ratiometric-based fluorescent probe does not depend on any external factors, which makes it a more attractive candidate for developing novel biosensors against heavy metals like zinc and for microscopic studies as well [22]. Therefore, a calibration curve was generated by plotting the ratio obtained from the fluorescence change at 495 and 520 nm, respectively (Fig. 9A). At the concentration of 3 μM Hg^{2+}, the increase in fluorescence [520/495 nm (F)] reached up to a maximum and then reached a plateau for FbFP$_{C56I}$, whereas in contrast, the wild-type FbFP was found to keep on increasing as the concentration of Hg^{2+} increases, as demonstrated in Fig. 9A. Furthermore, the ratio was found to be increasing in a linear fashion with Hg^{2+} from a range of 0.1–3 μM (Fig. 9B). This result demonstrates that the FbFP$_{C56I}$ can be used as a potential probe accompanied with distinct fluorescence changes for detecting the mercury ions at micromolar concentration with high sensitivity.

Although our limited mutational studies do not allow the exact identification of the nature of binding residues, they do not contradict the assumption that the mutation did not affect the protein chromophore formation and did also assist for mercury binding. Finally, our data analysis draws attention to the potential of the ratiometric method, which evidently describes a good relationship with respect to the Hg^{2+} concentration. Indeed, many chemosensors and fluorescent proteins-based mercury sensors are available, yet their ability of use for intracellular imaging purpose is limited to some other ways. Moreover, in recent times, a ratiometric probe is of great interest since it permits the calibration curve to be determined with respect to independence of the sample conditions, such as probe concentration and fluorescence intensity, and therefore can be useful for in vivo microscopic studies. Moreover, use of earlier reported fluorescence proteins can work only in the presence of aerobic conditions, which limit its applications towards anoxic conditions. Therefore, considering such above-mentioned challenges, the need to develop new fluorescent proteins is extremely important. In such regard, this reported new FMN class of fluorescent proteins as a ratiometric probe for detecting Hg^{2+} ions in micromolar range will be highly interesting. In addition, such findings will also address the major concern of using the fluorescent proteins as a metal sensor in anoxic conditions.

In conclusion, a reagentless sensing unit based on utilizing the metal-mediated fluorescence changes of FbFP has been successfully developed for quantitation of mercury ions. By exploring and engineering the residues near and around the FMN chromophore, we hereby report a first ratiometric-based fluorescent probe from the FMN class of proteins against the toxic heavy metal mercury. Furthermore, the results of the emission ratio observed from the engineered FbFP showed it can be utilized for measuring and monitoring the intracellular Hg^{2+} at low micromolar concentration under physiological pH conditions and most importantly will serve as an ideal reporter in cells with short oxygen supply. With the results obtained from this groundwork, further engineering of FbFP with metal-binding amino acids might open a new gateway for the development of various biosensors with high efficiency for detecting the heavy metals at contaminated environments and also help to understand the biology of metal ions in the field of anaerobic biology.

Acknowledgments

This research was partially supported by the Basic Science Research Program through the National Research Foundation of Korea (NRF) funded by the Ministry of Education, Science and Technology (NRF-2013R1A2A2A01068013), Korea and also from the Korean Health Technology R&D Project, Ministry of Health & Welfare, Republic of Korea (HN12C0055). Dr. Saravanan Prabhu Nadarajan was supported by the 2015 KU Brain Pool of Konkuk University.

References

1. Ayyadurai N, Saravanan Prabhu N, Deepankumar K, Lee SG, Jeong HH, Lee CS, Yun H. 2011. Development of a selective, sensitive, and reversible biosensor by the genetic incorporation of a metal-binding site into green fluorescent protein. *Angew. Chem. Int. Ed. Engl.* **50:** 6534-6537.
2. Balint EE, Petres J, Szabo M, Orban CK, Szilagyi L, Abraham B. 2013. Fluorescence of a histidine-modified enhanced green fluorescent protein (EGFP) effectively quenched by copper (II) ions. *J. Fluoresc.* **23:** 273-281.
3. Buckley AM, Petersen J, Roe AJ, Douce GR, Christie JM. 2015. LOV-based reporters for fluorescence imaging. *Curr. Opin. Chem. Biol.* **27:** 39-45.
4. Chapleau RR, Blomberg R, Ford PC, Sagermann M. 2008. Design of a highly specific and noninvasive biosensor suitable for real-time in vivo imaging of mercury (II) uptake. *Protein Sci.* **17:** 614-622.
5. Davis SJ, Vierstra RD. 1998. Soluble, highly fluorescent variants of green fluorescent protein (GFP) for use in higher plants. *Plant Mol. Biol.* **36:** 521-528.
6. Drepper T, Eggert T, Circolone F, Heck A, Krauss U, Guterl JK, *et al.* 2007. Reporter proteins for in vivo fluorescence without oxygen. *Nat. Biotechnol.* **25:** 443-445.
7. Ernst E. 2002. Toxic heavy metals and undeclared drugs in Asian herbal medicines. *Trends Pharmacol. Sci.* **23:** 136-139.
8. Giepmans BN, Adams SR, Ellisman MH, Tsien RY. 2006. The fluorescent toolbox for assessing protein location and function. *Science* **312:** 217-224.
9. Grandjean P, Weihe P, Nielsen F, Heinzow B, Debes F, Budtz-Jorgensen E. 2012. Neurobehavioral deficits at age 7 years associated with prenatal exposure to toxicants from maternal seafood diet. *Neurotoxicol. Teratol.* **34:** 466-472.
10. Grandjean P, Weihe P, White RF, Debes F, Araki S, Yokoyama K, *et al.* 1997. Cognitive deficit in 7-year-old children with prenatal exposure to methylmercury. *Neurotoxicol. Teratol.* **19:** 417-428.
11. Jiang T, Guo D, Wang Q, Wu X, Li Z, Zheng Z, *et al.* 2015. Developing a genetically encoded green fluorescent protein mutant for sensitive light-up fluorescent sensing and cellular imaging of Hg (II). *Anal. Chim. Acta* **876:** 77-82.
12. Kelly SM, Price NC. 2000. The use of circular dichroism in the investigation of protein structure and function. *Curr. Protein Pept. Sci.* **1:** 349-384.

13. Liu X, Jiang L, Li J, Wang L, Yu Y, Zhou Q, *et al.* 2014. Significant expansion of fluorescent protein sensing ability through the genetic incorporation of superior photo-induced electron-transfer quenchers. *J. Am. Chem. Soc.* **136:** 13094-13097.
14. Mackert JR, Jr., Berglund A. 1997. Mercury exposure from dental amalgam fillings: absorbed dose and the potential for adverse health effects. *Crit. Rev. Oral Biol. Med.* **8:** 410-436.
15. Masullo T, Puccio R, Di Pierro M, Tagliavia M, Censi P, Vetri V, *et al.* 2014. Development of a biosensor for copper detection in aqueous solutions using an *Anemonia sulcata* recombinant GFP. *Appl. Biochem. Biotechnol.* **172:** 2175-2187.
16. Mukherjee A, Walker J, Weyant KB, Schroeder CM. 2013. Characterization of flavin-based fluorescent proteins: an emerging class of fluorescent reporters. *PLoS One* **8:** e64753.
17. Mukherjee A, Weyant KB, Walker J, Schroeder CM. 2012. Directed evolution of bright mutants of an oxygen-independent flavin-binding fluorescent protein from *Pseudomonas putida*. *J. Biol. Eng.* **6:** 20.
18. Nadarajan SP, Ravikumar Y, Deepankumar K, Lee CS, Yun H. 2014. Engineering lead-sensing GFP through rational designing. *Chem. Commun. (Camb.)* **50:** 15979-15982.
19. Pudasaini A, El-Arab KK, Zoltowski BD. 2015. LOV-based optogenetic devices: light-driven modules to impart photoregulated control of cellular signaling. *Front. Mol. Biosci.* **2:** 18.
20. Rahimi Y, Shrestha S, Banerjee T, Deo SK. 2007. Copper sensing based on the far-red fluorescent protein, HcRed, from *Heteractis crispa*. *Anal. Biochem.* **370:** 60-67.
21. Ravikumar Y, Nadarajan SP, Lee CS, Rhee JK, Yun H. 2015. A new-generation fluorescent-based metal sensor – iLOV protein. *J. Microbiol. Biotechnol.* **25:** 503-510.
22. Taki M, Wolford JL, O'Halloran TV. 2004. Emission ratiometric imaging of intracellular zinc: design of a benzoxazole fluorescent sensor and its application in two-photon microscopy. *J. Am. Chem. Soc.* **126:** 712-713.
23. Tansila N, Tantimongcolwat T, Isarankura-Na-Ayudhya C, Nantasenamat C, Prachayasittikul V. 2007. Rational design of analyte channels of the green fluorescent protein for biosensor applications. *Int. J. Biol. Sci.* **3:** 463-470.
24. Tsien RY. 1998. The green fluorescent protein. *Annu. Rev. Biochem.* **67:** 509-544.
25. Verma N, Singh M. 2005. Biosensors for heavy metals. *Biometals* **18:** 121-129.
26. Wu J, Abdelfattah AS, Miraucourt LS, Kutsarova E, Ruangkittisakul A, Zhou H, *et al.* 2014. A long Stokes shift red fluorescent Ca^{2+} indicator protein for two-photon and ratiometric imaging. *Nat. Commun.* **5:** 5262.